

NOTICE: This is the author's version of a work accepted for publication by Elsevier. Changes resulting from the publishing process, including peer review, editing, corrections, structural formatting and other quality control mechanisms, may not be reflected in this document. Changes may have been made to this work since it was submitted for publication. A definitive version was subsequently published in Int. J. Hydrogen Energy, Vol. 35, 2010, 8446-8456, doi:10.1016/j.ijhydene.2010.05.098.

## **Hydrino Continuum Transitions with Cutoffs at 22.8 nm and 10.1 nm**

**R. L. Mills and Y. Lu**

BlackLight Power, Inc., 493 Old Trenton Road, Cranbury, NJ 08512

### **ABSTRACT**

Classical physical laws predict that atomic hydrogen may undergo a catalytic reaction with certain species, including itself, that can accept energy in integer multiples of the potential energy of atomic hydrogen,  $m \cdot 27.2$  eV, wherein  $m$  is an integer. The predicted reaction involves a resonant, nonradiative energy transfer from otherwise stable atomic hydrogen to the catalyst capable of accepting the energy. The product is  $H(1/p)$ , fractional Rydberg states of atomic hydrogen called "hydrino atoms," wherein  $n = 1/2, 1/3, 1/4, \dots, 1/p$  ( $p \leq 137$  is an integer) replaces the well-known parameter  $n = \text{integer}$  in the Rydberg equation for hydrogen excited states. Each hydrino state also comprises an electron, a proton, and a photon, but the field contribution from the photon increases the binding rather than decreasing it corresponding to energy desorption rather than absorption. Since the potential energy of atomic hydrogen is 27.2 eV, two H atoms formed from  $H_2$  by collision with a third, hot H can act as a catalyst for this third H by accepting  $2 \cdot 27.2$  eV from it. By the same mechanism, the collision of two hot  $H_2$  provide 3H to serve as a catalyst of  $3 \cdot 27.2$  eV for the fourth. Following the energy transfer to the catalyst an intermediate is formed having the radius of the H atom and a central field of 3 and 4 times the central field of a proton, respectively, due to the contribution of the photon of each intermediate. The radius is predicted to decrease as the electron undergoes radial acceleration to a stable state having a radius that is  $1/3$  ( $m = 2$ ) or  $1/4$  ( $m = 3$ ) the radius of the uncatalyzed hydrogen atom with the further release of 54.4 eV and 122.4 eV of energy, respectively. This energy emitted as a characteristic EUV continuum with a cutoff at 22.8 nm and 10.1 nm, respectively, was observed from pulsed hydrogen discharges. The continua spectra

directly and indirectly match significant celestial observations.

Key Words: hydrogen plasmas, catalysis, 22.8 nm and 10.1 nm EUV continua

## I. Introduction

J. R. Rydberg showed that all of the spectral lines of atomic hydrogen were given by a complete empirical relationship:

$$\bar{\nu} = R \left( \frac{1}{n_f^2} - \frac{1}{n_i^2} \right) \quad (1)$$

where  $R = 109,677 \text{ cm}^{-1}$ ,  $n_f = 1, 2, 3, \dots$ ,  $n_i = 2, 3, 4, \dots$  and  $n_i > n_f$ . Bohr, Schrödinger, and Heisenberg, each developed a theory for atomic hydrogen that gave the energy levels in agreement with Rydberg's equation.

$$E_n = -\frac{e^2}{n^2 8\pi\epsilon_0 a_H} = -\frac{13.598 \text{ eV}}{n^2} \quad (2a)$$

$$n = 1, 2, 3, \dots \quad (2b)$$

where  $e$  is the elementary charge,  $\epsilon_0$  is the permittivity of vacuum, and  $a_H$  is the radius of the hydrogen atom. Classical laws predict a reaction involving a resonant, nonradiative energy transfer from otherwise stable atomic hydrogen to a catalyst capable of accepting the energy to form hydrogen in lower-energy states than previously thought possible. The excited energy states of atomic hydrogen are given by Eq. (2a) for  $n > 1$  in Eq. (2b). The  $n = 1$  state is the “ground” state for “pure” photon transitions (i.e. the  $n = 1$  state can absorb a photon and go to an excited electronic state, but it cannot release a photon and go to a lower-energy electronic state). However, an electron transition from the ground state to a lower-energy state may be possible by a resonant nonradiative energy transfer such as multipole coupling or a resonant collision mechanism.

The theory reported previously [1–13] predicts that atomic hydrogen may undergo a catalytic reaction with certain atoms, excimers, ions, and diatomic hydrides such as  $\text{He}^+$ ,  $2\text{H}$ ,  $\text{Ar}^+$ ,  $\text{Sr}^+$ ,  $\text{Li}$ ,  $\text{K}$ ,  $\text{Cs}$ , and  $\text{NaH}$ , which provide a reaction with a net enthalpy of an integer multiple of the potential energy of atomic hydrogen,  $E_h = 27.2 \text{ eV}$ , where  $E_h$  is one Hartree. Specific species identifiable on the basis of their known electron energy levels are required to be present with atomic hydrogen to catalyze the process. The reaction involves a nonradiative energy transfer followed by continuum emission or energy transfer to H to form extraordinarily hot,

excited-state H [14–27] and a hydrogen atom that is lower in energy than unreacted atomic hydrogen that corresponds to a fractional principal quantum number given by

$$n = 1, \frac{1}{2}, \frac{1}{3}, \frac{1}{4}, \dots, \frac{1}{p}; \quad p \leq 137 \text{ is an integer} \quad (2c)$$

in Eq. (1). The  $n = 1$  state of hydrogen and the  $n = \frac{1}{\text{integer}}$  states of hydrogen are nonradiative,

but a transition between two nonradiative states, say  $n = 1$  to  $n = 1/2$ , is possible via a nonradiative energy transfer. Thus, a catalyst provides a net positive enthalpy of reaction of  $m \cdot 27.2$  eV (i.e. it resonantly accepts the nonradiative energy transfer from hydrogen atoms and releases the energy to the surroundings to affect electronic transitions to fractional quantum energy levels). As a consequence of the nonradiative energy transfer, the hydrogen atom becomes unstable and emits further energy until it achieves a lower-energy nonradiative state having a principal energy level given by Eqs. (2a) and (2c). Each hydrino state  $H(1/p)$  also comprises an electron, a proton, and a photon, but the field contribution from the photon increases the binding rather than decreasing it corresponding to energy desorption rather than absorption. The classical solutions of excited states and hydrino states are given in Ref. [1].

The data from a broad spectrum of investigational techniques strongly and consistently support the existence of these states called hydrino, for “small hydrogen,” and the corresponding diatomic molecules called molecular hydrino. Some of these prior related studies supporting the possibility of a novel reaction of atomic hydrogen, which produces hydrogen in fractional quantum states that are at lower energies than the traditional “ground” ( $n = 1$ ) state, include extreme ultraviolet (EUV) spectroscopy, characteristic emission from catalysts and the hydride ion products, lower-energy hydrogen emission, chemically-formed plasmas, Balmer  $\alpha$  line broadening, including in microwave plasmas with no electric field, population inversion of H lines, elevated electron temperature, anomalous plasma afterglow duration, power generation, and analysis of novel chemical compounds [14–46].

We recently reported the results on the  $\text{He}^+$  and  $2\text{H}$  catalyst systems, each providing a net enthalpy of reaction of 54.4 eV which is equivalent to  $2 \cdot 27.2$  eV [14]. The energy transfer to  $\text{He}^+$  was predicted to pump the  $\text{He}^+$  ion energy levels and increase the electron excitation temperature of H in helium-hydrogen and hydrogen plasmas, respectively. Following the energy transfer to the catalyst, the radius of the H atom is predicted to decrease as the electron

undergoes radial acceleration to a stable state having a radius that is  $1/3$  the radius of the uncatalyzed hydrogen atom with the further release of 54.4 eV of energy. This energy may be emitted as a characteristic EUV continuum with a cutoff at 22.8 nm and extending to longer wavelengths, or as third-body kinetic energy, wherein a resonant kinetic-energy transfer to form fast H occurs. Subsequent excitation of these fast  $H(n=1)$  atoms by collisions with the background species followed by emission of the corresponding  $H(n=3)$  fast atoms is predicted to give rise to broadened Balmer  $\alpha$  emission. The product  $H(1/3)$  reacts rapidly to form  $H(1/4)$ , then molecular hydrino,  $H_2(1/4)$ , as a preferred state. EUV spectroscopy and high-resolution visible spectroscopy were recorded on microwave and glow and pulsed discharges of helium with hydrogen and hydrogen alone. Pumping of the  $He^+$  ion lines occurred with the addition of hydrogen, and the excitation temperature of hydrogen plasmas under certain conditions was very high. Furthermore, for both plasmas providing catalysts  $He^+$  and  $2H$ , respectively, the EUV continuum and extraordinary ( $>50$  eV) Balmer  $\alpha$  line broadening were observed.

Gases from the pulsed-plasma cells showing continuum radiation were collected and dissolved in  $CDCl_3$ . Molecular hydrino  $H_2(1/4)$  was observed by solution NMR at the predicted chemical shift of 1.25 ppm on these, as well as gases collected from multiple plasma sources including helium-hydrogen, water-vapor-assisted hydrogen, hydrogen, and so-called rt-plasmas involving an incandescently heated mixture of strontium, argon, and hydrogen [14]. These results are in good agreement with prior results on synthetic reactions to form hydrino compounds comprising hydrinos. The  $^1H$  MAS NMR value of 1.13 ppm observed for  $H_2(1/4)$  in solid  $NaH \cdot F$  corresponded to the solution value of 1.2 ppm and that of gases from plasma cells having a catalyst. The corresponding hydrino hydride ion  $H^-(1/4)$  was observed from solid compounds at the predicted shift of  $-3.86$  ppm in solution NMR and its ionization energy was confirmed at the predicted energy of 11 eV by X-ray photoelectron spectroscopy [15, 16, 42, 44–46].

The basis of each signature can be understood from a more detailed understanding of the mechanism of the hydrino transition. Hydrogen is a special case of the stable states given by Eqs. (2a) and (2c), wherein the corresponding radius of the hydrogen or hydrino atom is given by

$$r = \frac{a_H}{p}, \quad (3)$$

where  $p = 1, 2, 3, \dots$ . In order to conserve energy, energy must be transferred from the hydrogen atom to the catalyst in units of

$$m \cdot 27.2 \text{ eV}, \quad m = 1, 2, 3, 4, \dots \quad (4)$$

and the radius transitions to  $\frac{a_H}{m+p}$ . Thus, the general reaction is given by

$$m \cdot 27.2 \text{ eV} + \text{Cat}^{q+} + \text{H} \left[ \frac{a_H}{p} \right] \rightarrow \text{Cat}^{(q+r)+} + re^- + \text{H} \left[ \frac{a_H}{(m+p)} \right] + [(m+p)^2 - p^2] \cdot 13.6 \text{ eV} \quad (5)$$

$$\text{Cat}^{(q+r)+} + re^- \rightarrow \text{Cat}^{q+} + m \cdot 27.2 \text{ eV} \quad (6)$$

And, the overall reaction is

$$\text{H} \left[ \frac{a_H}{p} \right] \rightarrow \text{H} \left[ \frac{a_H}{(m+p)} \right] + [(m+p)^2 - p^2] \cdot 13.6 \text{ eV} \quad (7)$$

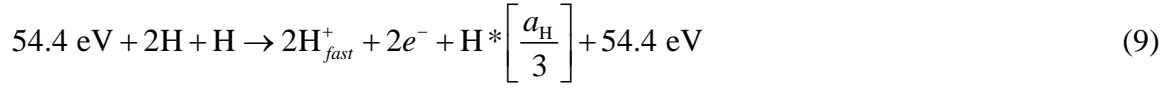
$q$  and  $r$  are integers.

As given in Chp. 5 of Ref [1], and Refs. [14, 15, 38], hydrogen atoms  $\text{H}(1/p)$   $p = 1, 2, 3, \dots, 137$  can undergo transitions to lower-energy states given by Eqs. (2a) and (2c), wherein the transition of one atom is catalyzed by a second that resonantly and nonradiatively accepts  $m \cdot 27.2 \text{ eV}$  with a concomitant opposite change in its potential energy. The overall general equation for the transition of  $\text{H}(1/p)$  to  $\text{H}(1/(m+p))$  induced by a resonance transfer of  $m \cdot 27.2 \text{ eV}$  to  $\text{H}(1/p')$  is represented by

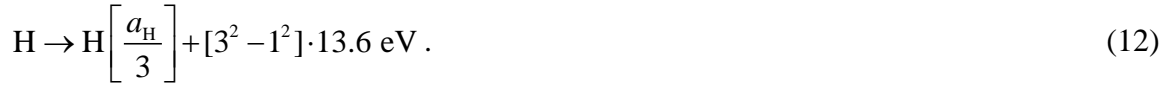
$$\text{H}(1/p') + \text{H}(1/p) \rightarrow \text{H} + \text{H}(1/(m+p)) + [2pm + m^2 - p'^2 + 1] \cdot 13.6 \text{ eV} \quad (8)$$

Thus, hydrogen atoms may serve as a catalyst wherein  $m = 1$  and  $m = 2$  for one and two atoms, respectively, acting as a catalyst for another. The rate for the two-atom-catalyst case would be appreciable only when the H density is high. But, a three-body H interaction is easily achieved when two H atoms arise with the collision of a hot H with  $\text{H}_2$ . This event can commonly occur in plasmas having a large population of extraordinarily fast H as reported previously [14–26]. This is evidenced by the unusual intensity of atomic H emission. In such cases, energy transfer can occur from a hydrogen atom to two others within sufficient proximity, being typically a few angstroms [Chp 6 of Ref. 1]. Then, the reaction between three hydrogen atoms, whereby two

atoms resonantly and nonradiatively accept 54.4 eV from the third hydrogen atom such that  $2H$  serves as the catalyst, is given by



And, the overall reaction is



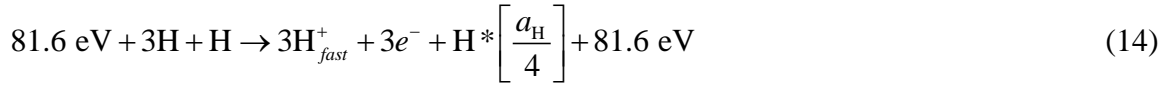
$H^*\left[\frac{a_H}{2+1}\right]$  has the radius of the hydrogen atom (corresponding to the 1 in the denominator) and a central field equivalent to 3 times that of a proton, and  $H\left[\frac{a_H}{3}\right]$  is the corresponding stable state with the radius of 1/3 that of H. As the electron undergoes radial acceleration from the radius of the hydrogen atom to a radius of 1/3 this distance, energy is released as characteristic light emission or as third-body kinetic energy. The emission may be in the form of an extreme-ultraviolet continuum radiation having an edge at 54.4 eV (22.8 nm) and extending to longer wavelengths. Alternatively, H is the lightest atom; thus, it is the most probable fast species in collisional energy exchange from the H intermediate (e.g.  $H^*\left[\frac{a_H}{2+1}\right]$ ). Additionally, H is unique with regard to the energetic transition state intermediate (generally represented by  $H^*\left[\frac{a_H}{m+p}\right]$ ) in that all these species are energy states of hydrogen with corresponding harmonic frequencies. Thus, the cross section for H excitation by a nonradiative energy transfer to form fast H is predicted to be large since it is a resonant process. Efficient energy transfer can occur by common through-space mechanisms such as dipole-dipole interactions as described by Förster's theory [Chp. 6, Ref.1]. Consequently, in addition to radiation, a resonant kinetic-energy transfer to form fast H may occur. Subsequent excitation of these fast  $H(n=1)$  atoms by collisions with the background  $H_2$  followed by emission of the corresponding  $H(n=3)$  fast

atoms gives rise to broadened Balmer  $\alpha$  emission. Extraordinary ( $>100$  eV) Balmer  $\alpha$  line broadening is observed consistent with predictions [14–26]. Indeed, the EUV continuum radiation, pumping of H excited states, and fast H were observed with hydrogen plasmas wherein 2H served as the catalyst [14]. Thus, the predictions corresponding to transitions of atomic hydrogen to form hydrinos was experimentally confirmed.

The predicted product 2H (Eqs. (9-12)) catalyst reaction is  $H(1/3)$ . In the case of a high hydrogen atom concentration, the further transition given by Eq. (8) of  $H(1/3)$  ( $p = 3$ ) to  $H(1/4)$  ( $m + p = 4$ ) with H as the catalyst ( $p' = 1$ ;  $m = 1$ ) can be fast:



In another H-atom catalyst reaction involving a direct transition to  $\left[ \frac{a_H}{4} \right]$  state, two hot  $H_2$  molecules collide and dissociate such that three H atoms serve as a catalyst of  $3 \cdot 27.2$  eV for the fourth. Then, the reaction between four hydrogen atoms, whereby three atoms resonantly and nonradiatively accept 81.6 eV from the fourth hydrogen atom such that 3H serves as the catalyst, is given by



And, the overall reaction is



The extreme-ultraviolet continuum radiation band due to the  $H^* \left[ \frac{a_H}{3+1} \right]$  intermediate of Eq. (14) is predicted to have short-wavelength cutoff at 122.4 eV (10.1 nm) and extend to longer wavelengths. In general, the transition of H to  $H \left[ \frac{a_H}{p = m + 1} \right]$  due by the acceptance of

$m \cdot 27.2$  eV gives a continuum band with a short-wavelength cutoff and energy  $E_{\left(\text{H} \rightarrow \text{H} \left[ \frac{a_{\text{H}}}{p=m+1} \right] \right)}$

given by

$$\begin{aligned} E_{\left(\text{H} \rightarrow \text{H} \left[ \frac{a_{\text{H}}}{p=m+1} \right] \right)} &= m^2 \cdot 13.6 \text{ eV} \\ \lambda_{\left(\text{H} \rightarrow \text{H} \left[ \frac{a_{\text{H}}}{p=m+1} \right] \right)} &= \frac{91.2}{m^2} \text{ nm} \end{aligned} \quad (18)$$

and extending to longer wavelengths than the corresponding cutoff.

In a previous publication, we reported the continuum radiation with a short-wavelength cutoff of 22.8 nm due to the decay of the intermediate corresponding to the hydrino state H(1/3) [14]. Molybdenum (Mo) electrodes were used in this study. The vapor pressure of Mo at T=2400 K is 0.0189 Pa; whereas, the vapor pressure of tungsten (W) and tantalum (Ta) are  $1.59 \times 10^{-6}$  Pa and  $5.21 \times 10^{-7}$  Pa, respectively, at this temperature [47]. The high metal vapor pressure with a Mo anode shorts the voltage and decreases the energy of the plasma species. It was observed that a minimum energy is required to cause the hydrino transitions as shown by the absence of significant continuum radiation below 10 kV. The plasma was also optically thick in that no strong metal lines were observed at the short wavelengths (<22 nm). In time-resolved studies using a channel electron multiplier detector and a multichannel scalar counter, the continuum emission was only observed during the short pulse; whereas, oxygen ions showed a long afterglow [48]. For example, the continuum at 25.0 nm had a short lifetime of about 0.5  $\mu$ s compared to 4  $\mu$ s lifetime of the O<sup>3+</sup> ion line at 23.9 nm. Thus, the observation of O ion lines in the absence of strong metal ion lines or continuum radiation was deemed to be due to the long O ion excited-state lifetimes relative to those of the continuum radiation or the optically thick, metal-ion-rich plasma. Since the recording time was orders of magnitude longer than the pulse time, the long-lived O ion radiation following decay of the attenuation of the optically thick metal ion plasma contributed disproportionately to the spectral intensity. In this paper, we report on the observation of an additional continuum band from the decay of the intermediate corresponding to the hydrino state H(1/4) by using different electrode materials that maintain a high voltage, optically-thin plasma during the short pulse discharge.

## II. Experimental Method

The experimental setup for recording the EUV spectra of pulsed plasmas using Mo, Ta, and W electrodes is shown in Fig. 1. EUV spectroscopy was recorded on argon, helium, pure hydrogen, and noble gas-hydrogen high-voltage pulsed discharge plasmas with a McPherson grazing incidence EUV spectrometer (Model 248/310G) equipped with a grating having 1200 lines/mm or a grating having 600 lines/mm. The angle of incidence was  $87^\circ$ . The wavelength region recorded by the monochromator was 10-30 nm (1200 lines/mm grating) or 5-45 nm (600 lines/mm grating). The wavelength resolution was about 0.05 nm (FWHM) with an entrance slit width of  $<1 \mu\text{m}$ . In order to avoid saturation of the detector, the EUV light was detected by a CCD detector (Andor iDus) cooled at  $-60^\circ\text{C}$  that replaced the CEM of prior studies [14].

The main discharge cell comprised a hollow anode (3 mm bore) and a hollow cathode (3 mm bore). Electrodes of W and Ta replaced Mo to eliminate metal emission as the source of continuum radiation and to observe a potentially wider continuum spectral range. The electrodes were separated by a 3 mm gap. A negative high-voltage DC power supply was used to apply -10 kV or -15 kV between the cathode and anode wherein a bank of ten 5200 pF capacitors were connected in parallel to this high-voltage source. The -15 kV was applied in repeat runs to determine any high-energy electron effect on the spectral profile. An electron gun (Clinton Displays, Part # 2-001), driven by a high-voltage pulse generator (DEI, PVX 4140), provided a pulsed electron beam with a beam voltage of 1-3 kV and a duration of 0.5 ms. The electron beam triggered a high-voltage pulsed discharge at a repetition rate of 5 Hz. The CCD detector was gated synchronously with the e-beam trigger. It had an exposure time of 100 ms for each pulse discharge comprising a breakdown time of about 300 ns. Each spectrum comprised the superposition of 500 discharges using the grating having 1200 lines/mm and 1000 discharges using the grating having 600 lines/mm. The CCD dark count was subtracted from the accumulated spectrum. Ultra-high purity argon, helium, hydrogen, and noble gas-hydrogen mixtures were flowed at rates between 1 and 10 sccm and pressures between 100 mTorr and 1300 mTorr controlled by a mass flow controller (MKS). On-line mass spectroscopy and high-resolution visible spectroscopy using the Jobin Yvon Horiba 1250 M spectrometer [14] ruled out contaminants in the plasma gasses.

### III. Results and Discussion

High purity argon (Fig. 2) and high purity helium (dashed traces of Figs. 3–8) were run as controls. The expected known argon and helium ion lines were observed in the absence of any continuum. Oxygen ion lines were also observed similarly in all spectra due to the oxide coat on the metal electrodes. In contrast, the predicted continua were observed for 2H and 3H as catalysts. The emission spectra of electron-beam-initiated, high-voltage pulsed discharges in pure hydrogen recorded by the EUV grazing incidence spectrometer with Mo, W, and Ta electrodes are shown in Figs. 3–5, respectively. The predicted continua from the transitions  $\text{H}^* \left[ \frac{a_{\text{H}}}{3} \right] \rightarrow \text{H} \left[ \frac{a_{\text{H}}}{3} \right] + 54.4 \text{ eV}$  and  $\text{H}^* \left[ \frac{a_{\text{H}}}{4} \right] \rightarrow \text{H} \left[ \frac{a_{\text{H}}}{4} \right] + 122.4 \text{ eV}$  were observed with a cutoff at 22.8 nm and 10.1 nm, respectively, with the intensity increasing to a maximum at longer wavelengths. Only, the 22.8 nm continuum was observed with Mo electrodes (Fig. 3); whereas, the 22.8 nm continuum and additionally the 10.1 nm continuum were observed with W and Ta electrodes (Figs. 4 and 5). Strong metal ion lines were also observed with the Mo electrodes having the highest metal vapor pressure of the metals tested. Metal absorption of short-wavelengths and reemission corresponding to an optically thick plasma could also be a contributing factor to the high intensity metal ion emission.

On-line mass spectroscopy and high-resolution visible spectroscopy confirmed that there were no gas contaminants. The 22.8 nm continuum was observed for Mo, W, and Ta electrodes, the 10.1 nm continuum was observed with both the W and Ta electrodes, no continuum was observed for plasmas absent hydrogen, and the continuum was observed in the noble gasses as hydrogen was added. Beginning at trace levels, the intensity was proportional to the H concentration (Fig. 9). Thus, the lines could not be due to electrode metal emission. Evidence of optical thickness is that no Mo metal lines were observed at short wavelengths (<22 nm) as shown in Fig. 3. Thus, the cutoff of the shorter-wavelength spectrum with Mo electrodes is expected, and the extraordinarily low volatility of W and Ta overcomes this limitation to permit the observation of both continua as shown in Figures 4 and 5. These metals also have a lower background in the helium controls since they hydride to a much less extent as was evidenced by the lower hydrogen off gassing following an H<sub>2</sub> run.

The recording of the spectra was repeated using a 600 lines/mm grating that gave a higher intensity than the 1200 lines/mm grating. The number of superpositions per spectrum was

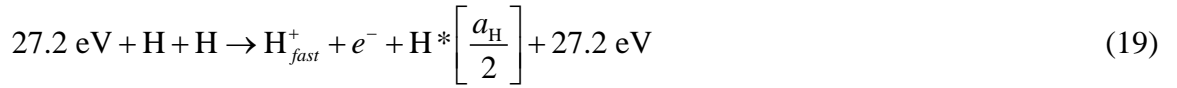
also increased from 500 to 1000. As shown in Fig. 6, the Mo electrode spectrum now showed both continua, the 10.1 nm in addition to the 22.8 nm. This confirmed that the plasma was optically thick in the case of Mo electrode. Thus, the optical thickness was overcome with the 600 line/mm grating. This result with those using Ta and W electrodes demonstrated that the same spectral features were observed with three electrode metals, eliminating any possibility that the spectra were due to metal emission. The spectra for all three electrodes readily showed the 22.8 nm short-wavelength cutoff, and the W and Ta spectra clearly showed the short-wavelength cutoff at 10.1 nm upon spectral magnification. As shown in Figs. 7 and 8, the 600 lines/mm grating clearly showed the 10.1 nm cutoff even on the same intensity scale as the control helium spectrum showing the strong helium ion lines. The continuum radiation is very intense, especially considering that the line emission intensity is concentrated into a narrow peak; whereas, the continuum is over a much larger wavelength range.

These results cannot be explained by conventional mechanisms. Ion recombination known to produce a continuum gives a characteristic “wedge” on a logarithmic plot of intensity versus wavelength wherein the electron temperature can be determined from the slope. The intensity for an ion recombination mechanism must be a maximum at the threshold and decrease exponentially to shorter wavelengths due to conservation of the energy of the recombination and the electron kinetic energy. In contrast, the profiles predicted for the decay of the intermediates corresponding to the hydrino states H(1/3) (Eq. (10)) and H(1/4) (Eq. 15)) have a short-wavelength cutoff with a maximum at longer wavelengths matching the observed profiles. Furthermore, the gas showing continua was pure hydrogen that has no recombination threshold at 22.8 nm or 10.1 nm. In fact, hydrogen has no Rydberg or molecular emission in the EUV region at all.

Bremsstrahlung was eliminated since Bremsstrahlung radiation has an intensity profile that exponentially decays from the long to short-wavelength region [49], and energetic electrons as the source was directly eliminated by the observation that changing the high voltage from -10 kV to -15 kV had no effect on the spectral profile. Additionally, molecules cannot emit in this energy region and were eliminated from consideration. Only atomic and ionic emission is possible at these energies corresponding to line emission, and no continuum emission is possible even for Doppler or Stark broadened lines. From Wien’s displacement law, blackbody radiation even at 24 nm wavelengths would correspond to a temperature of  $1.2 \times 10^5$  K, an absolutely

impossible scenario. Thus, the lines are assigned to predicted  $q \cdot 13.6$  eV continua with thresholds at 54.4 eV ( $q = 4$ ) (2H catalyst) and 122.4 eV ( $q = 9$ ) (3H catalyst).

We previously reported a 91.2 nm continuum in an argon plasma with trace hydrogen where the catalyst reaction  $\text{Ar}^+$  to  $\text{Ar}^{2+}$  has a net enthalpy of reaction of 27.63 eV, which is equivalent to  $m = 1$  in Eq. (18) [43]. Two hydrogen atoms may react to give the same continuum band by a reaction similar to those given by Eqs. (9)–(12). The reaction whereby one H resonantly and nonradiatively accepts 27.2 eV from the other hydrogen atom such that it serves as the catalyst, is given by



And, the overall reaction is



The emission from Eq. (20) may be in the form of an extreme-ultraviolet continuum radiation having an edge at 13.6 eV (91.2 nm) and extending to longer wavelengths. This band was also observed in pulsed pure hydrogen plasmas using the normal incidence spectrometer, but temporal studies are required in order to eliminate the background hydrogen molecular band. These bands were eliminated previously in the argon plasma with trace hydrogen [14, 43] wherein H is highly dissociated. Considering the 91.2 nm continuum shown in Figs. 17 and 31 of Ref. [43] and the results shown in Figs. 3–8, hydrogen may emit the series of 10.1 nm, 22.8 nm, and 91.2 nm continua.

Stars also comprise plasmas of hydrogen, and it is anticipated that some may emit these features. The emission from white dwarfs arising from an extremely high concentration of hydrogen is modeled as an optically thick blackbody of  $\sim 50,000$  K gas comprising predominantly hydrogen and helium. A modeled composite spectrum of the full spectral range from 10 nm to  $>91.2$  nm with an abundance  $\text{He}/\text{H}=10^{-5}$  from Barstow and Holberg [50] is shown in Fig. 10. Albeit, white dwarf spectra can be curve fitted using stratification and adjustable He

and H column densities and ionization fractions to remove some inconsistencies between optical and EUV spectra [51] and independent measurements of the latter, matching the spectrum at the short-wavelengths is problematic. Alternatively, combining the emission shown in Figs. 3–8 with the 91.2 nm continuum, observed previously [43], gives a spectrum with continua having edges at 10.1 nm, 22.8, nm, and 91.2 nm, a match to the white dwarf spectrum. However, the proposed nature of the plasmas and the mechanisms are very different. The emission in our studies is assigned to hydrino transitions in cold gas and optically-thin plasmas absent any helium. White-dwarf and celestial models may need revision and benefit from our discovery of high-energy H continua emission.

For example, there is no existing physical model that can couple the temperature and density conditions in different discrete regions of the outer atmosphere (chromosphere, transition region, and corona) of coronal/chromospheric sources [50]. Typically the corona is modeled to be three orders of magnitude hotter than the surface that is the source of coronal heating seemingly in defiance of the second law of thermodynamics. Reconciliation is offered by the mechanism of line absorption and re-emission of the  $m^2 \cdot 13.6$  eV (Eq. (18)) continuum radiation. The 91.2 nm continuum to longer wavelengths is expected to be prominent and is observed in the solar extreme ultraviolet spectrum as shown in Fig. 11 [52], despite attenuation by the coronal gas. As shown in Fig. 11, the continuum was greatly reduced in the prominence and the corona wherein the H concentration was much reduced and absent, respectively. The emission from chromospheric lines and the continuum was also severely attenuated in the corona. The strongest lines in the coronal spectrum and to a lesser extent the prominence are multiply ionized ions such as the doublets of Ne VIII, Mg X, or Si XII that could be due to absorption of high-energy continuum radiation rather than thermal excitation. High-energy-photon excitation is more plausible than a thermal mechanism with  $T \sim 10^6$  given the 4000 K surface temperature and the observation of the CO absorption band at 4.7  $\mu\text{m}$  in the solar atmosphere, wherein CO cannot exist above 4000 K [54]. Considering the 10.1 nm band as a source, the upper limit of coronal temperature based on excitation of about  $10^6$  K is an energy match. In addition to the temperature, another extraordinary observation is that although the total average energy output of the outer layers of the Sun is  $\cong 0.01$  % of the photospheric radiation, local transient events can produce an energy flux that exceeds the photospheric flux [55]. The energy source of the latter may be magnetic in nature, but identity of the highly

ionizing coronal source is not established. Nor has the total energy balance of the Sun been reconciled. The possibility of a revolutionary discovery of a new source of energy in the Sun based on a prior undiscovered process is an open question [56].

In the case that the medium is optically thick over certain wavelength regions, only parts of the broad emission may be observed. In addition, the continuum radiation may be indirectly observed as highly-ionized ion emission not consistent with a thermal origin in terms of the ions and intensity ratios. The emission depends on atomic and ion cross sections for energy exchange with hydrino intermediates and for absorption and reemission of the continuum radiation as well as the incident continuum profile. The latter is dependent on the hydrino reactions that are in turn also depend on the medium wherein a species other than H may serve as the catalyst [14, 36–38, 57–61].

Evidence for EUV emission from hydrino transitions also comes from interstellar medium (ISM) since it provides a source of the diffuse ubiquitous EUV cosmic background. Specifically, the 10.1 nm continuum matches the observed intense 11.0-16.0 nm band [50, 62]. Furthermore, it provides a mechanism for the high ionization of helium of the ISM and the excess EUV radiation from galaxy clusters that cannot be explained thermally [63]. Additional astrophysical evidence such as the observation that a large component of the baryonic matter of the universe is in the form of WHIM (warm-hot ionized media) in the absence of a conventional source and the match of hydrinos to the identity of dark matter was presented previously [14]. The latter case is further supported by observations of signature electron-positron annihilation energy.

Dark matter comprises a majority of the mass of the universe as well as intra-galactic mass [64, 65]. It would be anticipated to concentrate at the center of the Milky Way galaxy due to the high gravity from the presence of a super massive blackhole at the center that emits gamma rays as matter falls into it. Since hydrinos are each a state of hydrogen having a proton nucleus, high-energy gamma rays impinging on dark matter will result in pair production. The characteristic signature of the identity of dark matter as hydrino being the emission of the 511 keV annihilation energy of pair production is observed [66–68]. Another hydrino decay pathway for this radiation is given in Chp. 32 of Ref. [1]. Interstellar medium [69–71], gamma-ray bursts [71, 72], and the solar flares [55, 71, 73] also emit 511 keV line radiation. The dominant source of positrons in gamma-ray bursts is likely pair production by photon on photons or on strong

magnetic fields [71]. The solar-flare emission is likely due to production of radioactive positron emitters in accelerated charge interactions [71]; whereas, the diffuse 511 keV radiation by interstellar medium is consistent with the role of hydrino as dark matter in pair production from incident cosmic radiation [69–71].

### III. Conclusion

In this paper, we report on the extension of the range of continuum radiation from hydrino transitions with the observation of an additional continuum band from the decay of the intermediate corresponding to the hydrino state  $H(1/4)$ . By using different electrode materials of extremely low vapor pressure that maintain a high voltage, optically-thin plasma during the short pulse discharge, the radiation due to transitions due to 2H catalyst and 3H catalyst capable of accepting the energy to form hydrinos were observed.

For both catalysts, the energy due to the electron undergoing a radial transition to occupy a state of nearer radius was observed spectroscopically as a characteristic EUV continuum with a cutoff at 22.8 nm and 10.1 nm, respectively, that extended to longer wavelengths. The continuum radiation with a short-wavelength cutoff of 22.8 nm was observed with both W and Ta electrodes as well as Mo electrodes, but additionally, the predicted continuum radiation with a short-wavelength cutoff of 10.1 nm due to the decay of the intermediate corresponding to the hydrino state  $H(1/4)$  was observed with W and Ta electrodes. The latter was also seen with Mo by increasing the spectral signal. Thus, with electrodes that maintain high-voltage plasmas that are optically thin, continuum radiation from H plasma is observed in the entire region from 10.1 nm to at least 40 nm. Our laboratory experiments have celestial implications. Hydrogen continua from transitions to form hydrinos matches the emission from white dwarfs, provides a possible mechanism of linking the temperature and density conditions of the different discrete layers of the coronal/chromospheric sources, and provides a source of the diffuse ubiquitous EUV cosmic background with the 10.1 nm continuum matching the observed intense 11.0-16.0 nm band in addition to resolving other cosmological mysteries [14, 50, 62].

### References

1. R. Mills, *The Grand Unified Theory of Classical Physics*; June 2008 Edition, posted at <http://www.blacklightpower.com/theory/bookdownload.shtml>.

2. R. L. Mills, B. Holverstott, B. Good, N. Hogle, A. Makwana, "Total Bond Energies of Exact Classical Solutions of Molecules Generated by Millsian 1.0 Compared to Those Computed Using Modern 3-21G and 6-31G\* Basis Sets," *Phys. Essays* 23 (2010) 153-199; doi: 10.4006/1.3310832.
3. W. Xie, R.L. Mills, W. Good, A. Makwana, B. Holverstott and N. Hogle, "Millsian 2.0: A Molecular Modeling Software for Structures, Charge Distributions and Energetics of Biomolecules," submitted for publication.
4. R. L. Mills, "Classical Quantum Mechanics," *Phys. Essays*, 16 (2003) 433-498.
5. R. Mills, "Physical Solutions of the Nature of the Atom, Photon, and Their Interactions to Form Excited and Predicted Hydrino States," *Phys. Essays*, 20 (2007) 403-460.
6. R. L. Mills, "Exact Classical Quantum Mechanical Solutions for One- Through Twenty-Electron Atoms," *Phys.s Essays*, 18 (2005), 321-361.
7. R. L. Mills, "The Nature of the Chemical Bond Revisited and an Alternative Maxwellian Approach," *Phys. Essays*, 17 (2004) 342-389.
8. R. L. Mills, "Maxwell's Equations and QED: Which is Fact and Which is Fiction," *Phys. Essays*, 19 (2006) 225-262.
9. R. L. Mills, "Exact Classical Quantum Mechanical Solution for Atomic Helium Which Predicts Conjugate Parameters from a Unique Solution for the First Time," *Phys. Essays*, 21 (2008) 103-141.
10. R. L. Mills, "The Fallacy of Feynman's Argument on the Stability of the Hydrogen Atom According to Quantum Mechanics," *Annales de la Fondation Louis de Broglie*, 30, No. 2, (2005) 129-151.
11. R. Mills, "The Grand Unified Theory of Classical Quantum Mechanics," *Int. J. Hydrogen Energy*, 27 (2002) 565-590.
12. R. Mills, "The Nature of Free Electrons in Superfluid Helium—a Test of Quantum Mechanics and a Basis to Review its Foundations and Make a Comparison to Classical Theory," *Int. J. Hydrogen Energy*, 26 (2001) 1059-1096.
13. R. Mills, "The Hydrogen Atom Revisited," *Int. J. of Hydrogen Energy*, 25 (2000) 1171-1183.
14. R. L. Mills, Y. Lu, K. Akhar, "Spectroscopic Observation of Helium-Ion- and Hydrogen-Catalyzed Hydrino Transitions," *Cent. Eur. J. Phys.*, (2009), doi: 10.2478/s11534-009-0106-9.

15. R. L. Mills, G. Zhao, K. Akhtar, Z. Chang, J. He, Y. Lu, W. Good, G. Chu, B. Dhandapani, "Commercializable Power Source from Forming New States of Hydrogen," *Int. J. Hydrogen Energy*, 34 (2009) 573-614.
16. R. Mills, P. Ray, B. Dhandapani, W. Good, P. Jansson, M. Nansteel, J. He, A. Voigt, "Spectroscopic and NMR Identification of Novel Hydride Ions in Fractional Quantum Energy States Formed by an Exothermic Reaction of Atomic Hydrogen with Certain Catalysts," *Eur. Phys. J.-Appl. Phys.*, 28 (2004) 83-104.
17. K. Akhtar, J. Scharer, R. L. Mills, Substantial Doppler broadening of atomic-hydrogen lines in DC and capacitively coupled RF plasmas, *J. Phys. D, Appl. Phys.*, 42 (2009) 42 135207 (2009) doi:10.1088/0022-3727/42/13/135207.
18. R. Mills, K. Akhtar, "Tests of Features of Field-Acceleration Models for the Extraordinary Selective H Balmer  $\alpha$  Broadening in Certain Hydrogen Mixed Plasmas," *Int. J. Hydrogen Energy* 34 (2009) 6465-6477.
19. R. L. Mills, P. Ray, B. Dhandapani, R. M. Mayo, J. He, "Comparison of Excessive Balmer  $\alpha$  Line Broadening of Glow Discharge and Microwave Hydrogen Plasmas with Certain Catalysts," *J. Appl. Phys.*, 92, (2002) 7008-7022.
20. R. L. Mills, P. Ray, B. Dhandapani, J. He, "Comparison of Excessive Balmer  $\alpha$  Line Broadening of Inductively and Capacitively Coupled RF, Microwave, and Glow Discharge Hydrogen Plasmas with Certain Catalysts," *IEEE Transactions on Plasma Science*, 31(2003) 338-355.
21. R. L. Mills, P. Ray, "Substantial Changes in the Characteristics of a Microwave Plasma Due to Combining Argon and Hydrogen," *New J. Phys.*, www.njp.org, 4 (2002) 22.1-22.17.
22. R. L. Mills, B. Dhandapani, K. Akhtar, "Excessive Balmer  $\alpha$  Line Broadening of Water-Vapor Capacitively-Coupled RF Discharge Plasmas," *Int. J. Hydrogen Energy*, 33 (2008) 802-815.
23. R. Mills, P. Ray, B. Dhandapani, "Evidence of an Energy Transfer Reaction Between Atomic Hydrogen and Argon II or Helium II as the Source of Excessively Hot H Atoms in RF Plasmas," *J. Plasma Phys.*, 72 (2006) 469-484.
24. J. Phillips, C-K Chen, K. Akhtar, B. Dhandapani, R. Mills, "Evidence of Catalytic Production of Hot Hydrogen in RF Generated Hydrogen/Argon Plasmas," *Int. J. Hydrogen Energy*, 32 (2007) 3010-3025.

25. R. L. Mills, P. C. Ray, R. M. Mayo, M. Nansteel, B. Dhandapani, J. Phillips, "Spectroscopic Study of Unique Line Broadening and Inversion in Low Pressure Microwave Generated Water Plasmas," *J. Plasma Phys.*, 71 (2005) 877-888.
26. R. L. Mills, K. Akhtar, Fast H in Hydrogen Mixed Gas Microwave Plasmas when an Atomic Hydrogen Supporting Surface Was Present, *Int. J. Hydrogen Energy*, 35 (2010) 2546-2555, doi:10.1016/j.ijhydene.2009.12.148.
27. R. Mills and M. Nansteel, P. Ray, "Argon-Hydrogen-Strontium Discharge Light Source," *IEEE Trans. Plasma Sci.*, 30 (2002) 639-653.
28. R. Mills and M. Nansteel, P. Ray, "Bright Hydrogen-Light Source due to a Resonant Energy Transfer with Strontium and Argon Ions," *New J. Phys.*, 4 (2002) 70.1-70.28.
29. R. Mills, J. Dong, Y. Lu, "Observation of Extreme Ultraviolet Hydrogen Emission from Incandescently Heated Hydrogen Gas with Certain Catalysts," *Int. J. Hydrogen Energy*, 25 (2000) 919-943.
30. R. Mills, M. Nansteel, and P. Ray, "Excessively Bright Hydrogen-Strontium Plasma Light Source Due to Energy Resonance of Strontium with Hydrogen," *J. Plasma Physics*, Vol. 69, (2003), pp. 131-158.
31. R. L. Mills, J. He, M. Nansteel, B. Dhandapani, "Catalysis of Atomic Hydrogen to New Hydrides as a New Power Source," *Int. J. Global Energy Issues*, Special Edition in Energy Systems, 28, Nos. 2/3 (2007) 304-324.
32. H. Conrads, R. Mills, Th. Wrubel, "Emission in the Deep Vacuum Ultraviolet from a Plasma Formed by Incandescently Heating Hydrogen Gas with Trace Amounts of Potassium Carbonate," *Plasma Sources Science and Technol.*, 12 (2003) 389-395.
33. R.L. Mills, K. Akhtar, G. Zhao, Z. Chang, J. He, X. Hu, G. Chu, "Commercializable Power Source Using Heterogeneous Hydrino Catalysts," *Int. J. Hydrogen Energy*, 35 (2010) 395-419, doi: 10.1016/j.ijhydene.2009.10.038.
34. J. Phillips, R. L. Mills, X. Chen, "Water Bath Calorimetric Study of Excess Heat in 'Resonance Transfer' Plasmas," *J. Appl. Phys.*, 96 (2004) 3095-3102.
35. R. L. Mills, X. Chen, P. Ray, J. He, B. Dhandapani, "Plasma Power Source Based on a Catalytic Reaction of Atomic Hydrogen Measured by Water Bath Calorimetry," *Thermochimica Acta*, 406/1-2 (2003) 35-53.

36. R. L. Mills, P. Ray, "Extreme Ultraviolet Spectroscopy of Helium-Hydrogen Plasma," J. Phys. D, Appl. Phys., 36 (2003) 1535-1542.
37. R. L. Mills, P. Ray, B. Dhandapani, M. Nansteel, X. Chen, J. He, "New Power Source from Fractional Quantum Energy Levels of Atomic Hydrogen that Surpasses Internal Combustion," J Mol. Struct., 643, No. 1-3 (2002) 43-54.
38. R. Mills, P. Ray, "Spectral Emission of Fractional Quantum Energy Levels of Atomic Hydrogen from a Helium-Hydrogen Plasma and the Implications for Dark Matter," Int. J. Hydrogen Energy, 27 (2002) 301-322.
39. R. Mills, P. Ray, R. M. Mayo, "CW HI Laser Based on a Stationary Inverted Lyman Population Formed from Incandescently Heated Hydrogen Gas with Certain Group I Catalysts," IEEE Trans. Plasma Sci., 31 (2003) 236-247.
40. R. L. Mills, P. Ray, "Stationary Inverted Lyman Population Formed from Incandescently Heated Hydrogen Gas with Certain Catalysts," J. Phys. D, Appl. Phys., 36 (2003) 1504-1509.
41. R. Mills, P. Ray, R. M. Mayo, "The Potential for a Hydrogen Water-Plasma Laser," Appl. Phys. Lett., 82 (2003) 1679-1681.
42. R. L. Mills, P. Ray, "A Comprehensive Study of Spectra of the Bound-Free Hyperfine Levels of Novel Hydride Ion  $H^{-}(1/2)$ , Hydrogen, Nitrogen, and Air," Int. J. Hydrogen Energy, 28 (2003) 825-871.
43. R. Mills, "Spectroscopic Identification of a Novel Catalytic Reaction of Atomic Hydrogen and the Hydride Ion Product," Int. J. Hydrogen Energy, 26 (2001) 1041-1058.
44. R. Mills, B. Dhandapani, M. Nansteel, J. He, T. Shannon, A. Echezuria, "Synthesis and Characterization of Novel Hydride Compounds," Int. J. of Hydrogen Energy 26 (2001) 339-367.
45. R. Mills, B. Dhandapani, M. Nansteel, J. He, A. Voigt, "Identification of Compounds Containing Novel Hydride Ions by Nuclear Magnetic Resonance Spectroscopy," Int. J. Hydrogen Energy, 26 (2001) 965-979.
46. R. Mills, B. Dhandapani, N. Greenig, J. He, "Synthesis and Characterization of Potassium Iodo Hydride," Int. J. of Hydrogen Energy, 25, (2000) 1185-1203.
47. D. R. Lide, *CRC Handbook of Chemistry and Physics*, 86th Edition, CRC Press, Taylor & Francis, Boca Raton, (2005-6), p. 4-130.

48. A. F. H. van Gessel, Masters Thesis: *EUV spectroscopy of hydrogen plasmas*, April (2009), Eindhoven University of Technology, Department of Applied Physics, Group of Elementary Processes in Gas Discharges, EPG 09-02, pp. 61-70.
49. V. Grishin, B. Ishkhanov, S. Lichachev, V. Petukhov, "Electron Recirculator as High Efficiency Source of Hard Radiation," Proceedings of EPAC 2000, Vienna, Austria, (2000), 2606–2608.
50. M. A. Barstow and J. B. Holberg, *Extreme Ultraviolet Astronomy*, Cambridge Astrophysics Series 37, Cambridge University Press, Cambridge, (2003).
51. M. A. Barstow and J. B. Holberg, *Extreme Ultraviolet Astronomy*, Cambridge Astrophysics Series 37, Cambridge University Press, Cambridge, (2003), Chp 8.
52. M. Stix, *The Sun*, Springer-Verlag, Berlin, (1991), Figure 9.5, p. 321.
53. E. M. Reeves, E. C. M. Huber, G. J. Timothy, "Extreme UV spectroheliometer on the Apollo telescope mount," *Appl. Optics*, 16 (1977) 837-848.
54. Phillips, J. H., *Guide to the Sun*, Cambridge University Press, Cambridge, Great Britain, (1992), pp. 126-127.
55. M. Stix, *The Sun*, Springer-Verlag, Berlin, (1991), pp. 351-356.
56. [http://nobelprize.org/nobel\\_prizes/physics/articles/bahcall/](http://nobelprize.org/nobel_prizes/physics/articles/bahcall/)
57. S. Labov, S. Bowyer, "Spectral observations of the extreme ultraviolet background," *The Astrophys. J.*, 371 (1991) 810-819.
58. S. Bower, G. Field, and J. Mack, "Detection of an anisotropic soft X-ray background flux," *Nature*, 217, (1968) 32.
59. C. W. Danforth, J. M. Shull, "The low- $z$  intergalactic medium. III. H I and metal absorbers at  $z < 0.4$ ," *Astrophys. J.*, 679 (2008) 194-219.
60. N. Werner, A. Finoguenov, J. S. Kaastra, A. Simionescu, J. P. Dietrich, J Vink, H. Böhringer, "Detection of hot gas in the filament connecting the clusters of galaxies Abell 222 and Abell 223," *Astron. Astrophys. Lett.*, 482 (2008) L29-L33.
61. N. Craig, M. Abbott, D. Finley, H. Jessop, S. B. Howell, M. Mathioudakis, J. Sommers, J. V. Vallerga, R. F. Malina, "The Extreme Ultraviolet Explorer stellar spectral atlas," *Astrophys. J. Suppl.*, 113 (1997) 131-193.
62. R. Stern, S. Bowyer, "Apollo-Soyuz survey of the extreme-ultraviolet/soft X-ray background," *Astrophys. J.*, 230 (1979), 755-767.

63. S. Bowyer, J. J. Drake, S. Vennes, "Extreme ultraviolet spectroscopy," *Ann. Rev. Astron. Astrophys.*, 38 (2000) 231-288.
64. F. Bournaud, P. A. Duc, E. Brinks, M. Boquien, P. Amram, U. Lisenfeld, B. Koribalski, F. Walter, V. Charmandaris, "Missing mass in collisional debris from galaxies," *Science*, 316 (2007) 1166–1169.
65. B. G. Elmegreen, "Dark matter in galactic collisional debris," *Science*, 316 (2007) 32-33.
66. P. Jean, J. Knödleseder, V. Lonjou, M. Allain, J.P. Roques, G.K. Skinner, et al., "Early SPI/INTEGRAL measurements of 511 keV line emission from the 4<sup>th</sup> quadrant of the Galaxy," *Astron. Astrophys.*, 407 (2003) L55-L58.
67. M. Chown, "Astronomers claim dark matter breakthrough," *NewScientist.com*, Oct. 3, (2003), <http://www.newscientist.com/article/dn4214-astronomers-claim-dark-matter-breakthrough.html>.
68. C. Boehm, D. Hooper, J. Silk, M. Casse, J. Paul, "MeV dark matter: Has it been detected," *Phys. Rev. Lett.*, 92, (2004) 101301.
69. G. H. Share, "Recent results on celestial gamma radiation from SMM," *Adv. Space Res.*, 11 (1991) 85-94.
70. G. H. Share, R. L. Kinzer, D. C. Messina, W. R. Purcell, E. L. Chupp, D. J. Forrest, E. Rieger, "Observations of galactic gamma-radiation with the SMM spectrometer," *Adv. Space Res.*, 6 (1986) 145-148.
71. B. Kozlovsky, R. E. Lingenfelter, R. Ramaty, "Positrons from accelerated particle interactions," *Astrophys. J.*, 316 (1987) 801-818.
72. E. P. Mazets, S. V. Golenetskii, V. N. Il'inskii, R. L. Aptekar', Y. A. Guryan, "Observations of a flaring X-ray pulsar in Dorado," *Nature*, 282 (1979) 587-589.
73. G. H. Share, E. L. Chupp, D. J. Forrest, E. Rieger in *Positron and Electron Pairs in Astrophysics*, ed. M. L. Burns, A. K. Harding, R. Ramaty, "Positron annihilation radiation from Solar flares," (1983), New York: AIP, pp. 15-20.

Figure 1. Experimental setup for the high-voltage pulsed discharge cell.

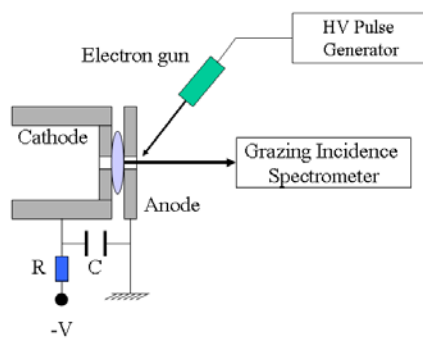
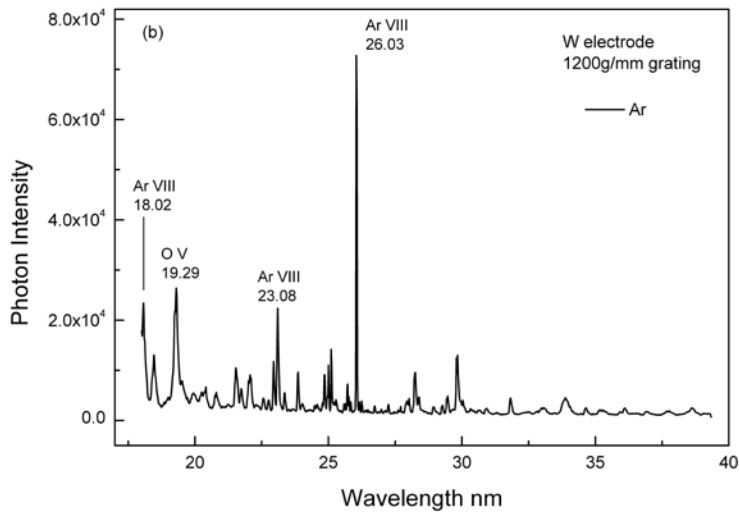
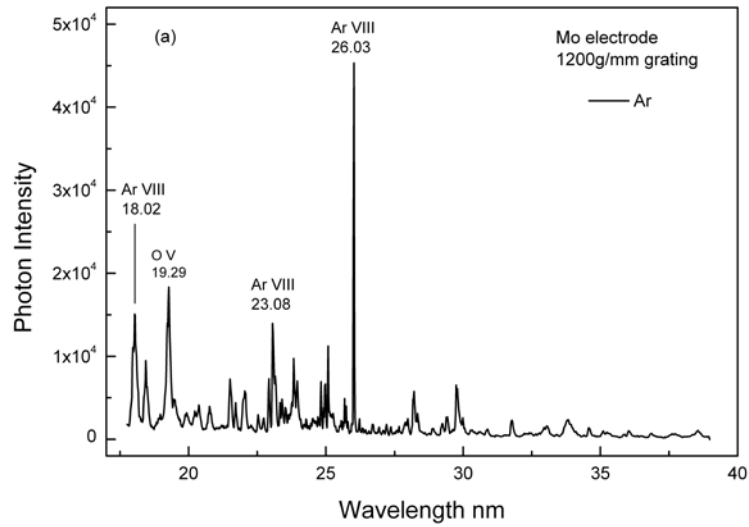


Figure 2. Emission spectrum (10 nm–35 nm) of an electron-beam-initiated, high-voltage pulsed discharge in argon recorded by the EUV grazing incidence spectrometer using the 1200 lines/mm grating and 500 superpositions. Only known argon and oxygen ion lines were observed in the absence of a continuum. (a) Mo electrodes. (b) W electrodes. (c) Ta electrodes.



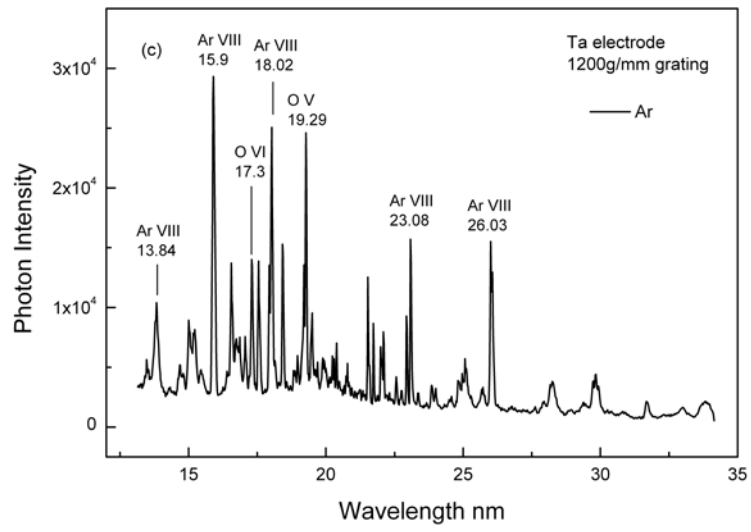


Figure 3. Emission spectra (17–38 nm) of electron-beam-initiated, high-voltage pulsed discharges in hydrogen (thick) and helium (thin) with Mo electrodes recorded by the EUV grazing incidence spectrometer using the 1200 lines/mm grating and 500 superpositions. The predicted continuum from the transition  $\text{H}^* \left[ \frac{a_{\text{H}}}{3} \right] \rightarrow \text{H} \left[ \frac{a_{\text{H}}}{3} \right] + 54.4 \text{ eV}$  was observed for hydrogen only. The sharp peaks are Mo and oxygen ions. The metal ion emission was attenuated at short-wavelengths.

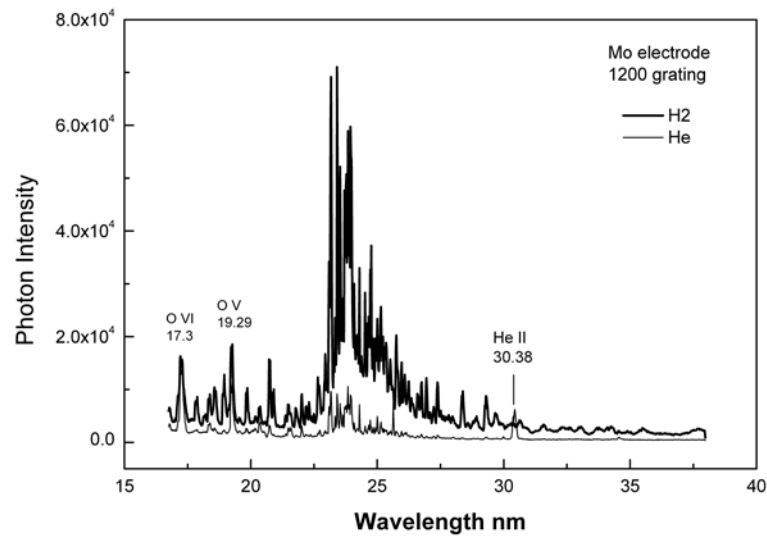


Figure 4. Emission spectra (12–33 nm) of electron-beam-initiated, high-voltage pulsed discharges in hydrogen (thick) and helium (thin) with W electrodes recorded by the EUV grazing incidence spectrometer using the 1200 lines/mm grating and 500 superpositions showing two continuum bands. The predicted continua from the transitions  $\text{H}^* \left[ \frac{a_{\text{H}}}{3} \right] \rightarrow \text{H} \left[ \frac{a_{\text{H}}}{3} \right] + 54.4 \text{ eV}$  and  $\text{H}^* \left[ \frac{a_{\text{H}}}{4} \right] \rightarrow \text{H} \left[ \frac{a_{\text{H}}}{4} \right] + 122.4 \text{ eV}$  were observed for hydrogen only. The sharp peaks are W and oxygen ions. The plasma was optically thin since the metal ion lines and continuum were not cut off at short-wavelengths.

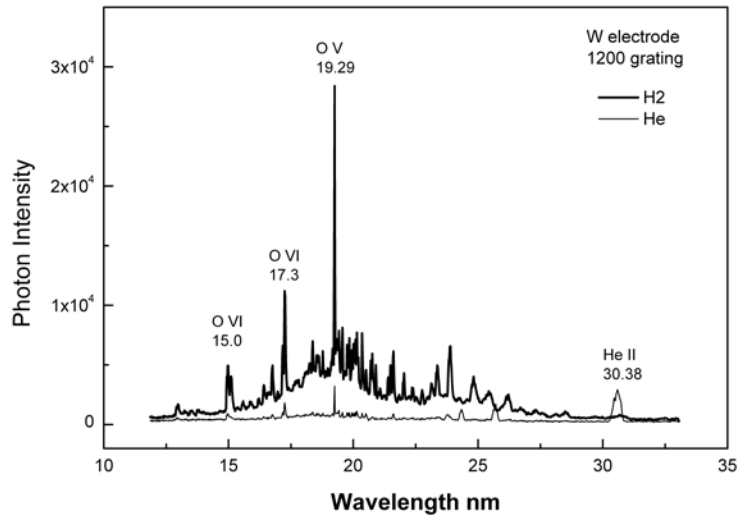


Figure 5. Emission spectra (10–31 nm) of electron-beam-initiated, high-voltage pulsed discharges in hydrogen (thick) and helium (thin) with Ta electrodes recorded by the EUV grazing incidence spectrometer using the 1200 lines/mm grating and 500 superpositions showing two continuum bands. The predicted continua from the transitions

$$\text{H}^* \left[ \frac{a_{\text{H}}}{3} \right] \rightarrow \text{H} \left[ \frac{a_{\text{H}}}{3} \right] + 54.4 \text{ eV} \quad \text{and} \quad \text{H}^* \left[ \frac{a_{\text{H}}}{4} \right] \rightarrow \text{H} \left[ \frac{a_{\text{H}}}{4} \right] + 122.4 \text{ eV}$$

were observed for hydrogen only. The sharp peaks are Ta and oxygen ions. The plasma was optically thin since the metal ion lines and continuum were not cut off at short-wavelengths.

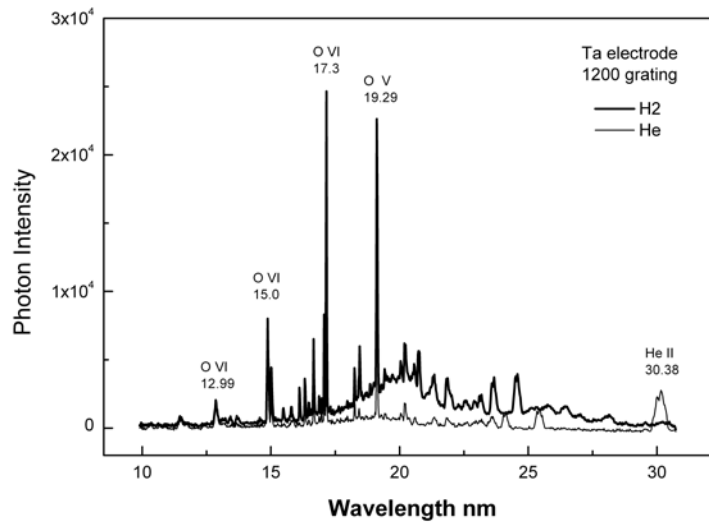


Figure 6. Emission spectra (3–46 nm) of electron-beam-initiated, high-voltage pulsed discharges in hydrogen (thick) and helium (thin) with Mo electrodes recorded by the EUV grazing incidence spectrometer using the 600 lines/mm grating and 1000 superpositions. In addition to the

predicted continuum from the transition  $H^* \left[ \frac{a_H}{3} \right] \rightarrow H \left[ \frac{a_H}{3} \right] + 54.4 \text{ eV}$ , the additional transition

$H^* \left[ \frac{a_H}{4} \right] \rightarrow H \left[ \frac{a_H}{4} \right] + 122.4 \text{ eV}$  was observed for hydrogen only due to the higher signal. The

same continuum bands were observed with all three metals wherein the optical thickness with Mo electrodes was overcome with higher signal.

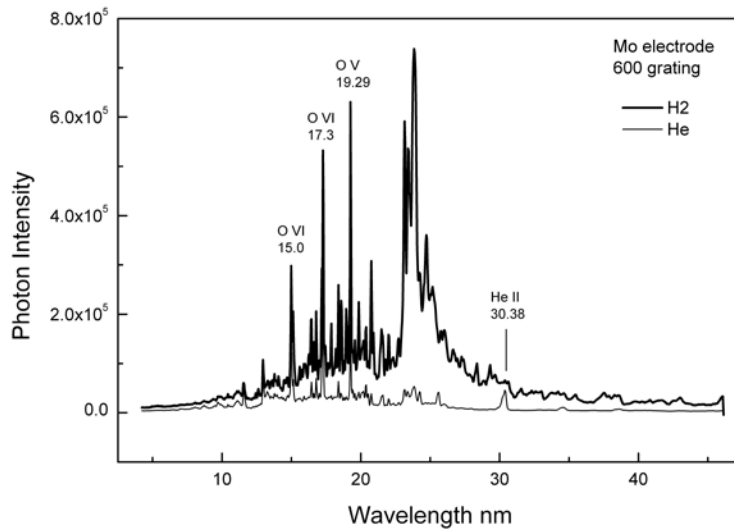


Figure 7. Emission spectra (3–46 nm) of electron-beam-initiated, high-voltage pulsed discharges in hydrogen (thick) and helium (thin) with W electrodes recorded by the EUV grazing incidence spectrometer using the 600 lines/mm grating and 1000 superpositions showing two continuum bands.

The predicted continua from the transitions  $H^* \left[ \frac{a_H}{3} \right] \rightarrow H \left[ \frac{a_H}{3} \right] + 54.4 \text{ eV}$  and

$H^* \left[ \frac{a_H}{4} \right] \rightarrow H \left[ \frac{a_H}{4} \right] + 122.4 \text{ eV}$  were observed for hydrogen only. The short-wavelength cutoffs

at cutoff at 22.8 nm and 10.1 nm were observed without spectral magnification.

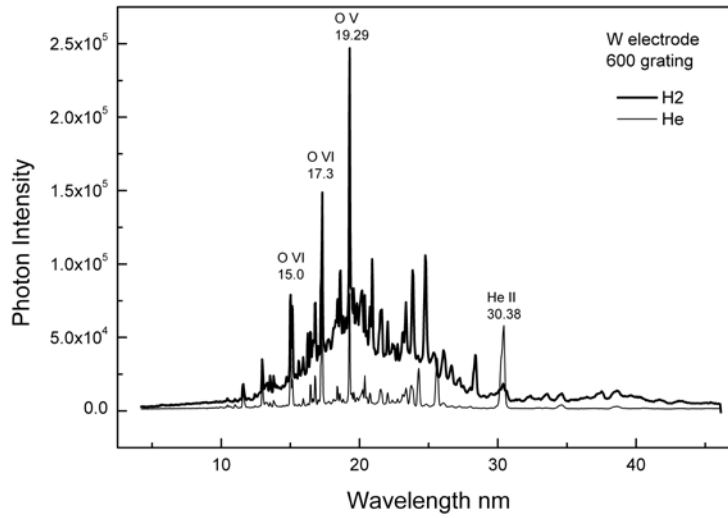


Figure 8. Emission spectra (3–46 nm) of electron-beam-initiated, high-voltage pulsed discharges in hydrogen (thick) and helium (thin) with Ta electrodes recorded by the EUV grazing incidence spectrometer using the 600 lines/mm grating and 1000 superpositions showing two continuum bands.

The predicted continua from the transitions  $\text{H}^* \left[ \frac{a_{\text{H}}}{3} \right] \rightarrow \text{H} \left[ \frac{a_{\text{H}}}{3} \right] + 54.4 \text{ eV}$  and

$\text{H}^* \left[ \frac{a_{\text{H}}}{4} \right] \rightarrow \text{H} \left[ \frac{a_{\text{H}}}{4} \right] + 122.4 \text{ eV}$  were observed for hydrogen only. The short-wavelength cutoffs

at cutoff at 22.8 nm and 10.1 nm were observed without spectral magnification.

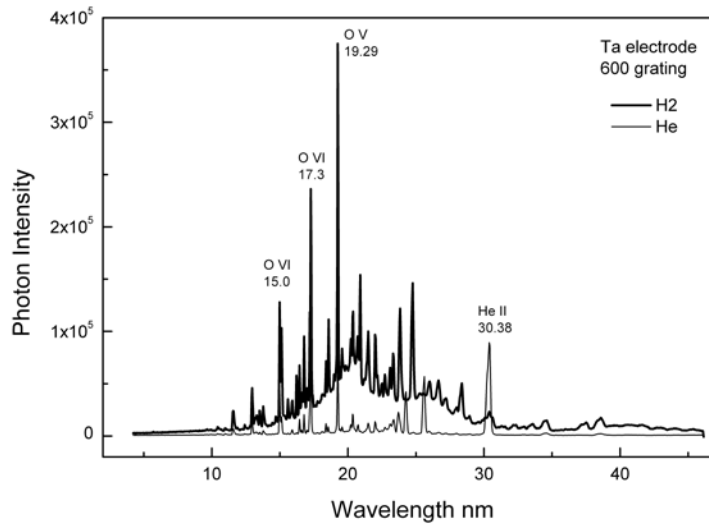


Figure 9. Emission spectra (10–35 nm) of electron-beam-initiated, high-voltage pulsed discharges in helium-hydrogen mixtures with W electrodes recorded by the EUV grazing incidence spectrometer using the 600 lines/mm grating and 1000 superpositions showing two continuum bands. The continua increased in intensity with increasing hydrogen pressure.

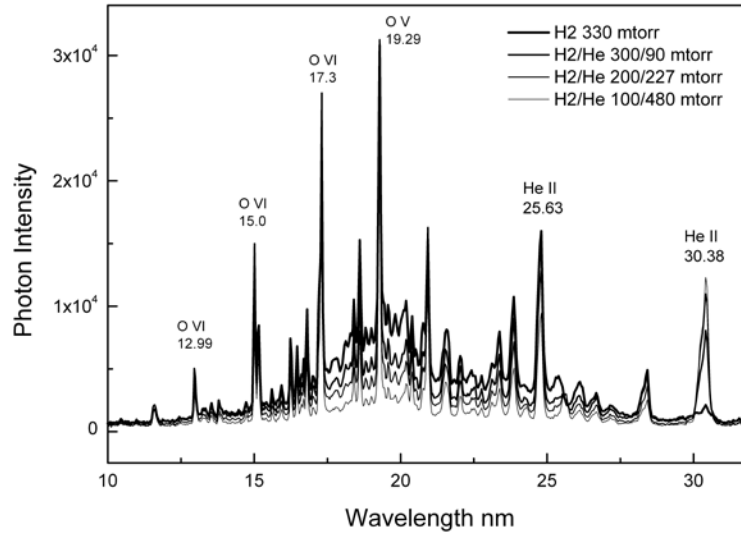


Figure 10. An exemplary model of the EUV continuum spectrum of the photosphere of a white dwarf using a temperature of 50,000 K and a number abundance of  $\text{He}/\text{H} = 10^{-5}$  showing the He II and H I Lyman absorption series of lines at 22.8 nm (228 Å) and 91.2 nm (912 Å), respectively. Reproduced by permission of Cambridge University Press [50].

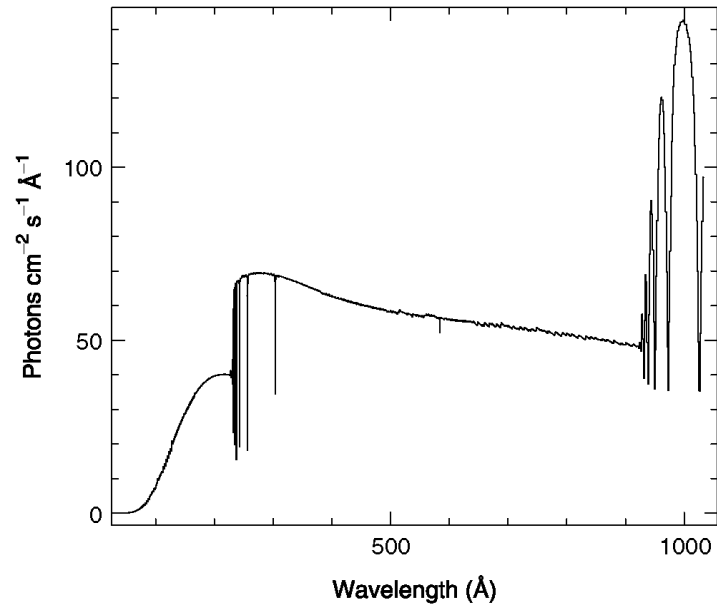


Figure 11. Skylab (Harvard College Observatory spectrometer) average extreme ultraviolet spectra of the Sun [52] recorded on a prominence (Top), quiet Sun-center (Middle), and corona above the solar limb (Bottom). From Reeves et al. [53].

